



## Finite Element Modelling of Non-Ductile RC Shear Walls Utilizing CFRP Sheets

Ibrahim K. Shaheen<sup>1</sup>, David T. Lau<sup>2</sup>, Carlos A. Cruz-Noguez<sup>3</sup>

<sup>1</sup>Graduate Student, Department of Civil and Environmental Engineering, Carleton University - Ottawa, ON, Canada.

<sup>2</sup>Professor, Department of Civil and Environmental Engineering, Carleton University - Ottawa, ON, Canada.

<sup>3</sup>Assistant Professor, Dept. of Civil and Environmental Engineering, University of Alberta - Edmonton, Alberta, Canada.

### ABSTRACT

The non-linear response behaviour of non-ductile Reinforced Concrete (RC) shear walls utilizing Carbon Fibre Reinforced Polymer (CFRP) sheets in retrofit and strengthening scenarios is presented. The analytical simulations are performed utilizing the finite element (FEM) program Vector 2. Analytical simulations presented include innovations on modelling techniques to account for the separation between the FRP and the concrete substrate due to the opening up of flexural cracks in the wall specimens (also known as intermediate crack de-bonding mechanism or IC de-bonding). In addition to modelling of the IC de-bonding mechanism along with FRP repair and strengthening applications, another novel modelling aspect included in this study is the ability to model the behaviour of lap spliced reinforcing bars through the use of bond stress-slip mechanisms in unconfined reinforced concrete shear walls. The analytical models detailed in this paper are validated using experimental results obtained from a recent experimental study of nine shear wall specimens with aspect ratio ranging from 0.65 to 1.20. The test specimens include a range of deficiencies of poor confinement, poor detailing, and the presence of lap spliced bars located in the plastic hinge region. Analytical results are shown to accurately portray the hysteresis behaviour of the wall specimens, along with relatively close predictions of the peak load, ultimate displacement, energy dissipation, and the associated failure mechanisms. The FRP sheets are shown to improve the ductility of the shear walls by delaying the initiation of failure in all test specimens and transitioning the failure behaviour of the walls to a more flexural ductile mechanism.

Keywords: Seismic Retrofit, Lap Splice Modelling, RC Shear Walls, IC-debonding, CFRP sheets.

### INTRODUCTION

Over the past four decades, the understanding of seismic design of reinforced concrete structures has evolved from primarily strength design criteria [1-2] to the consideration of both the strength and ductility of structures [3-4]. Although structures designed in accordance to current design standards generally perform well during earthquakes, there still exists a large stock of deficient shear wall structures designed using old obsolete design approach of strength design alone. In order to mitigate the seismic risk of these existing old shear wall structures, the retrofit method of using fibre reinforced polymers (FRP) sheets to repair and strengthen old deficient shear walls has attracted increasing attention in the last two decades [5-8]. On the modeling of FRP reinforced concrete structures, majority of the analytical investigations in the literature concern the modelling of FRP sheets in repair and strengthening of RC beams and slabs [9-11]. In comparison, relatively few reported analytical studies focus on the modelling of RC shear walls with externally bonded FRP sheets [12-14]. Most previous studies do not consider the de-bonding failure mechanism of the FRP material from the concrete substrate surface by either adopting the assumption of perfect bond or some simplified imperfect bond model [12-13]. The study conducted by Cruz-Noguez et al. [14], applied the concept of intermediate crack de-bonding (IC debonding) criteria in their model of the FRP debonding failure in shear wall simulations with vertically oriented FRP sheets in repair and strengthening applications. It has been pointed out by Teng et al. [15] through extensive experimental testing that the consideration of IC debonding has significant influence on the global structural response and mode of failure of FRP reinforced concrete beams. In addition to the experimental observations reported in [14-15] neglecting IC debonding leads to overestimation of the peak strength and ductility in the non-linear structural response of the simulation results. Furthermore on previous studies of deficient shear walls, which typically include insufficient shear and/or moment capacity, the defects of lack of confinement at the wall boundaries which prevents premature buckling of longitudinal reinforcing bars and the presence of lap splice of rebars in moment critical locations of the wall base have not been considered.

In this study, four squat shear wall specimens with an aspect ratio of 0.65, two of which include lap splice of lap splice length  $36d_b$  and  $21d_b$  at the plastic hinge location are modeled using the finite element program Vector 2 [16]. In this study, all wall specimens resist lateral loads predominantly by shear mechanisms. The wall specimens have a longitudinal reinforcement ratio of 3% and a transverse reinforcement ratio of 0.25% with no confinement detailing at the boundary elements of the walls. Because of space limitations only, the squat wall with  $21d_b$  lap splice length is shown in Figure 1. The details of the other wall specimens can be found in [17].

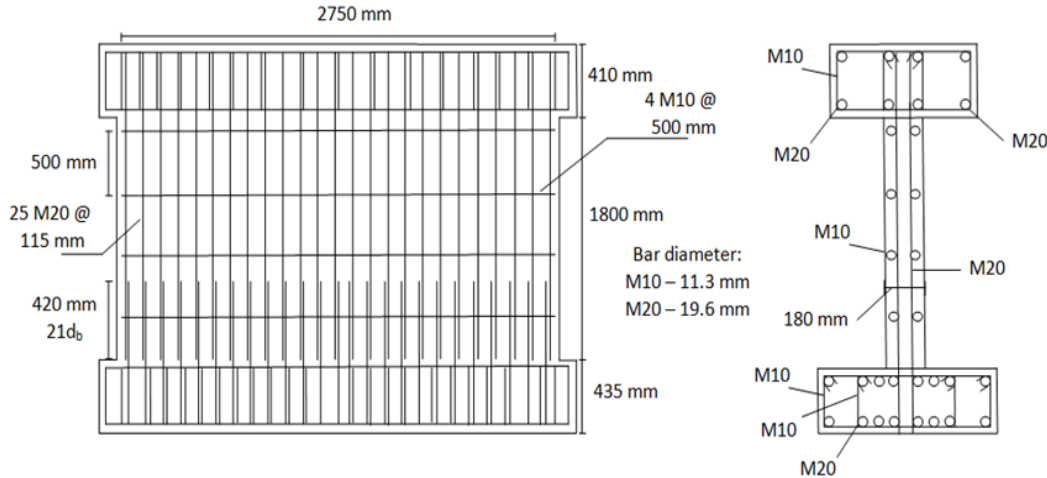


Figure 1. Shear wall geometric details (Squat Wall Specimen with  $21d_b$  Lap Splice)

Based on design assumptions which are verified later in finite element simulations, the control walls are expected to experience a brittle shear failure prior to reaching their ultimate flexural capacity. The FRP repair scheme (Table 1.) was designed in all cases to promote ductile flexural failure behaviour by increasing the shear capacity of the wall through the utilization of horizontal CFRP sheets to exceed beyond the flexural capacity of the wall. This would lead the wall to increase its lateral load resisting capacity to be governed by its flexural strength capacity and its deformation response to be more ductile.

Table 1. Repair Schemes (Per Side)

Wall I.D.	Specimen Type	State	Vertical FRP Sheets	Horizontal FRP Sheets
CW1†	Squat (No Lap Splice)	Control	-	-
RW1†	Squat (No Lap Splice)	Repaired	-	8
CW2†	Squat ( $21d_b$ Lap Splice)	Control	-	-
RW2	Squat ( $21d_b$ Lap Splice)	Repaired	-	8
CW3	Squat ( $36d_b$ Lap Splice)	Control	-	-
RW3	Squat ( $36d_b$ Lap Splice)	Repaired	-	8

† Specimens not tested to ultimate failure in Experimental Program

## IC DEBONDING CRITERIA & CRACK MODELLING APPROACH

Intermediate crack debonding is a phenomenon that is encountered when the FRP sheets debond from the concrete substrate surface due to the opening up of flexural cracks in the concrete [10]. Based on the observations reported in [10], the phenomenon is initiated with flexural cracking that quickly propagates to the laminate edges causing delamination or sag between the FRP and the cracked concrete, as the interfacial stresses between the concrete and the FRP sheets greatly exceed the bond stresses between the FRP and the concrete substrate. Sequential propagation of cracks causes FRP elements to debond quickly from the concrete causing a sudden drop in the load bearing capacity of the structural member. In this study, the IC debonding criteria are applied within a macro-scale finite element model in a smeared crack modeling approach [9], in which the concrete medium is treated as a continuum, and concrete cracking is represented by an infinite number of parallel cracks with infinitely small width that are smeared or evenly distributed over the element. In this approach, crack propagation is simulated by reducing the stiffness and strength of the concrete. The IC debonding criteria utilized is comprised of two bond stress-slip relationships that characterize the response of FRP-Concrete interaction. The first is a relationship obtained for regions with major flexural cracking, and the other being a relationship governing the response of the FRP-concrete bond in regions with no major flexural cracking. A major flexural crack is defined as a crack that is characterized by large slips that surpass the allowable slip limit, as shown in Figure 2. The allowable slip limit in this study follows the model proposed by Lu

et al. [10]. If a concrete element contains a flexural crack, the respective slips on the two sides of the flexural crack give the total interfacial slip within the interface element as the width of the flexural crack. Therefore the width of the crack needed to initiate IC debonding must be larger than  $2S_0$ , where  $S_0$  is the allowable slip limit. The derivations of the bond stress-slip relationships shown in Figure 2. are presented in [10]. The debonding criteria shown in Figure 2 are used in the models of the present study, to model the IC debonding failure of the CFRP sheets from the shearwall concrete substrate surface.

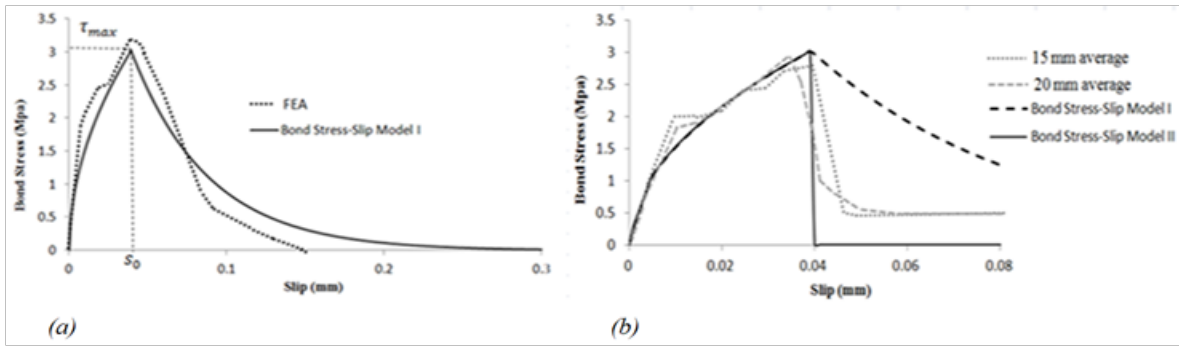


Figure 2. (a) Bond stress-slip curves for FRP-Concrete regions outside of major flexural crack zones; (b) Bond stress-slip curves for FRP-Concrete regions inside of major flexural crack zones. [Adapted from [10]]

### LAP SPICED BARS AND BOND MODELLING APPROACH

In addition to the IC debonding phenomenon presented previously, the modeling of lap-spliced longitudinal bars is investigated. Prior to the introduction of modern seismic design code provisions, the usage of lap spliced bars was permitted in moment critical locations, also known as plastic hinge locations. Observations of earthquake damage of concrete shear walls as well as analytical studies have shown that the lap splice of longitudinal rebars result in premature failure of shear wall structures with significant increase in non-ductile inelastic deformation in the response. The response of lap spliced reinforcing bars is mainly affected by two main factors relating to: (a) the amount of concrete confinement, and (b) the bonded length between lap spliced bars. However, even when sufficient lap splice length is provided, lap splices located in the plastic hinge region have been shown to slip [18]. Lap splice slippage can occur in two potential modes of failure: (a) Pull-out failure, and (b) Splitting failure. Pull-out failure occurs in confined concrete due to a pull out force exceeding the lap splice bearing capacity between the rebar ribs and the surrounding concrete material as shown in Figure 3. (a). Splitting failure on the other hand, occurs in unconfined concrete or mildly confined concrete, whereby a tensile splitting crack forms parallel to the ribs of the steel rebar and then subsequent cracking in the concrete keys and freedom of the bars to open up, leading to loss of all associated bearing capacity in the structure, as shown in Figure 3. (b). Many experimental bond stress-slip relationships for reinforcing bars in confined and unconfined concrete have been proposed to characterize the interaction behaviour of these elements in the literature [19-22]. It is a challenge to model lap splice behaviour in the non-linear behavior of lap spliced bars in unconfined concrete. The pull-out failure of lap splice rebars has been investigated in previous studies [19-20]. Lap splice modelling has been discussed in the literature [23-24]. Close agreement with experimental tests were reported in these previous studies. However in these previous studies, the effect of the lap splice contribution was modeled as contribution to the global response of the structure and not focusing on the local behaviour and failure of the lap splice. Assumptions were made on the stresses developed in the bars and the bonded area or confinement pressure. In this study, the lap splice contribution to the global response behaviour of shear walls is modeled using the methodology presented in [23], which utilizes a bond stress-slip relationship proposed in [22] to represent the nonlinear behaviour of lap spliced rebars. This modeling approach of lap spliced rebars has been verified to give close agreement with the test results reported in [25]. The bond model reported in [22] is derived based on regression analysis of test data from previous experimental studies of beam specimens reported in [21]. The beam specimens considered in [21] ranged from specimens with no confinement in the lap splice region to specimens with confinement in the form of stirrups, FRP fibres, and FRP strips. The model obtained from the experimental investigations contains three bond stress-slip curves as presented in Figure 4.

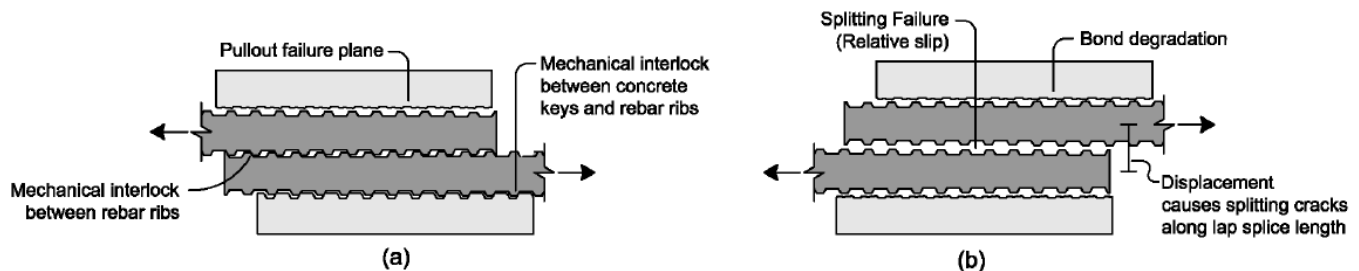


Figure 3. (a) Pull-out Failure Mode; (b) Splitting Failure Mode [Adapted from [30]]

The first curve represents the pull-out failure envelope which shows that the specimens considered had a good confinement behaviour of the concrete. The second curve represents the splitting failure criterion of mildly confined or unconfined concrete where the concrete experiences splitting failure due to the inability of the confinement pressure to prevent the opening up of the tensile cracks along the lap splice length. The third curve represents the plain concrete criteria which is similar to failure due to splitting.

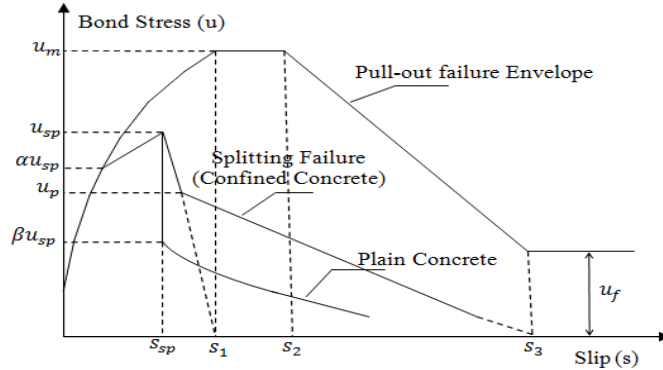


Figure 4. Local bond stress-slip relationship for different concrete confinement criteria [Adapted from [21]]

The derivations of the curves in (Figure 4.) are presented in [22]. The local bond stress-slip models shown in Figure 4 are utilized in the finite element simulations of the present study. The splitting failure bond model is the bond model selected to represent the bonding mechanism between the concrete medium and the lapped longitudinal rebars.

### GEOMETRIC MODELLING OF THE WALL SPECIMENS

The FE models for the wall specimens are modeled as shown in Figure 5. The wall specimens are modelled as a single concrete region which includes the longitudinal bars modelled as discrete truss elements, while the lateral reinforcement is smeared within the concrete region. The top link elements are assigned a very stiff bond to simulate perfect bonding conditions as these links represent the linkage of the wall panels to the cap beam. The links between the wall panel and the foundation block are modelled by inducing fixed supports on all nodes at the base restricting translational degrees of freedom in both the lateral and longitudinal directions. In the case of RW2, and RW3, this method in modelling is applied as a simplification to the modelling process, as large quantities of truss elements are present in the models for representing the horizontal FRP as well as the lap spliced bars (21d<sub>b</sub> and 36d<sub>b</sub>) modelled on top of each other.

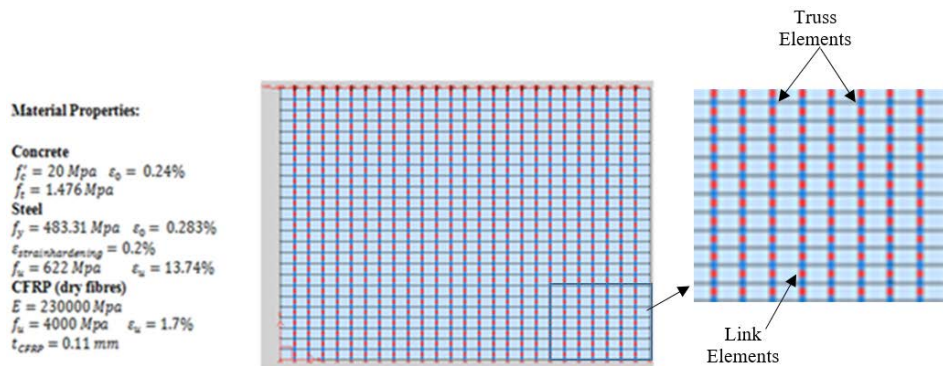


Figure 5. CW2 wall model

### MODELLING OF THE CONCRETE MEDIUM

Figure 5. shows the properties of the concrete used in this analytical study. For walls retrofitted with FRP sheets, the FRP reinforcement is attached externally on the faces of the wall specimen (not wrapped around the walls). This is adopted in the present study because of the consideration that it is difficult in field application to wrap FRP sheets around the shear wall panel. Thus the FRP is not considered to provide any confinement to the concrete medium. With regards to material models, the compression pre-peak response is characterized by the model proposed by Popovics et al. [26] for normal strength concrete. For the compression post-peak response, the Mander model [27] is selected. To model slip distortions between the steel elements and the concrete region, the slip distortion criteria by Vecchio and Lai [28] is selected. Concrete damage is

modelled by the damage model proposed by Palermo and Vecchio selecting the [29] of nonlinear loading and reloading hysteresis response model with decay.

### MODELLING OF STEEL REINFORCEMENT BARS & STIRRUPS

To model the stirrups, the reinforcement ratio is utilized to distribute the stirrups uniformly within the concrete region. The longitudinal bars in the model are represented as discrete truss elements connected to the concrete region through the use of a two dimensional zero length link element. The link element is composed of two orthogonal springs that connect the nodes of (continuous bars, lap splice bars and FRP sheets) to the concrete at the same coordinates (common node approach). The first spring tangential to the discrete truss element represents the bond stresses and bond slips and is equivalent in essence to a shear spring. The second spring deforms radially to the discrete truss element and represents the radial displacements and stresses and is equivalent to a flexural spring [16]. The failure criterion for the reinforcement bars is tensile fracture. Buckling of the longitudinal bars was considered by selecting the Asatsu model as the bars are modelled as discrete truss elements. Buckling of the lateral bars was not considered as they were smeared within the concrete region.

### MODELLING OF EXTERNALLY BONDED FRP SHEETS

The FRP sheets are represented in the model by a series of discrete truss elements made of an elastic brittle material with tension only capacity. The FRP is then linked to the concrete utilizing the common node approach. In the common node approach debonding does not occur between the FRP layers. Multiple layers of FRP sheets are included in the truss elements. Instead of modeling separately each layer of truss elements, a single layer of truss elements with a total area of all FRP layers is represented. This methodology is applied in the modelling process as Vector 2 [16], limits the maximum number of elements that can be used in the FE analysis, making the modeling of 8 layers of FRP truss elements on top of each other unfeasible. The properties of the dry fibre material are shown in Figure 5. as reported by woods et al. [30]. The failure mode of the FRP material is considered to occur when the maximum tensile capacity of the FRP is exceeded. A unique feature of Vector 2 is the ability to activate (engage) unstressed elements and deactivate (disengage) stressed elements on demand during the analysis while still keeping track of the damage contracted by the concrete elements during each loading stage. This feature is utilized in all wall specimens retrofitted with CFRP sheets.

### ANALYTICAL REPAIR PROCEDURE BACKGROUND

The repair procedure is simulated by activating/deactivating layers of reinforcement trusses that are bonded to the initial reinforced concrete region. If a layer of inactive FRP trusses is attached to the concrete panel, the FRP trusses can be activated in a later condition to simulate repair by accounting for the previously stressed state of the previously active element layers. The repaired walls are analyzed by superimposing mesh layers of an initially inactive and later active discrete FRP truss layer on the main concrete region. The control wall specimens are analyzed until the panel is just at the onset of failure. Then the FRP sheets are fully engaged and the wall specimens are then analyzed without stoppage until ultimate failure. Through this simulation process, the stress states of the concrete are retained when overlain with the CFRP sheets in repair simulations.

### FEM RESULTS & DISCUSSION

The wall specimens are subjected to a displacement controlled reverse cyclic loading up to failure. It is to be noted, that some wall specimens were not tested to failure. This was done to ensure a more practical repair scenario for repair of the damaged walls [30]. Comparison between the experimental and simulation results on hysteresis behaviour are presented in Figures 6 and 7. Due to space limitations, the failure modes of the lap-spliced walls are presented in Figures 8 and 9, and the parametric results are summarized in *Table 2*.

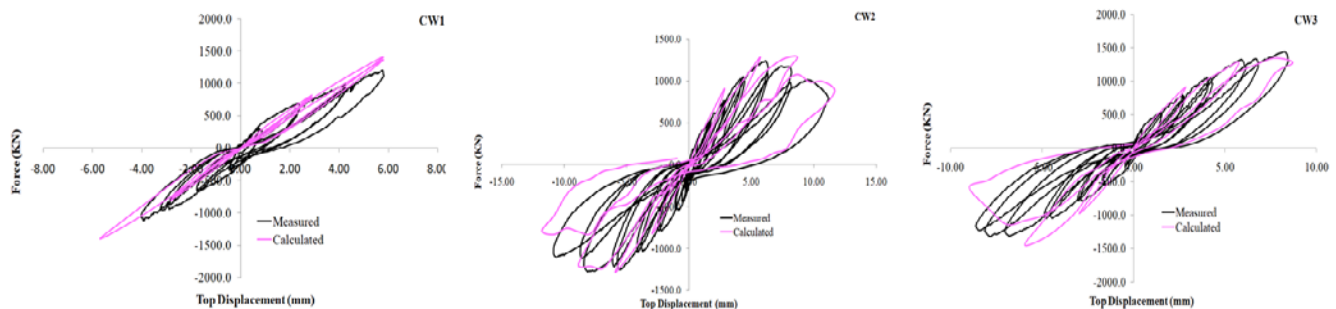


Figure 6. Control Wall Specimens Calculated vs. Measured Hysteresis Plots

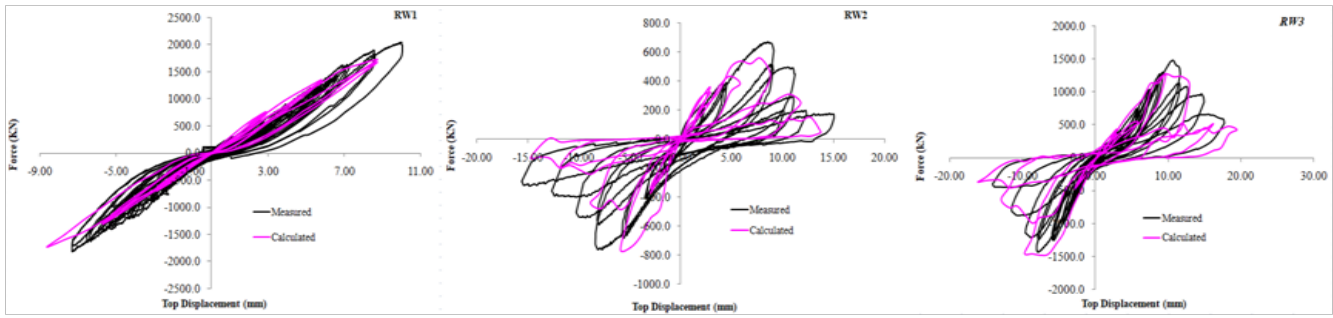


Figure 7. Repaired Wall Specimens Calculated vs. Measured Hysteresis Plots

Table 2. Calculated vs. Measured Parameters

Wall I.D.	Initial Stiffness Measured (kN/mm)	Initial Stiffness Calculated (kN/mm)	Max. Load Measured (kN)	Max. Load Calculated (kN)	Ult. Disp. Measured (mm)	Ult. Disp. Calculated (mm)	Ult. Drift Measured (%)	Ult. Drift Calculated (%)
CW1	367	330	1205	1407	5.81	5.71	0.32	0.30
RW1	271	263	1980	1734	8.67	8.61	0.48	0.48
CW2	426	376	1240	1284	10.1	10.7	0.56	0.59
RW2	125	184	715	656	10.6	11.2	0.59	0.62
CW3	420	408	1390	1344	8.50	8.70	0.47	0.48
RW3	200	203	1460	1440	11.2	12.9	0.62	0.72

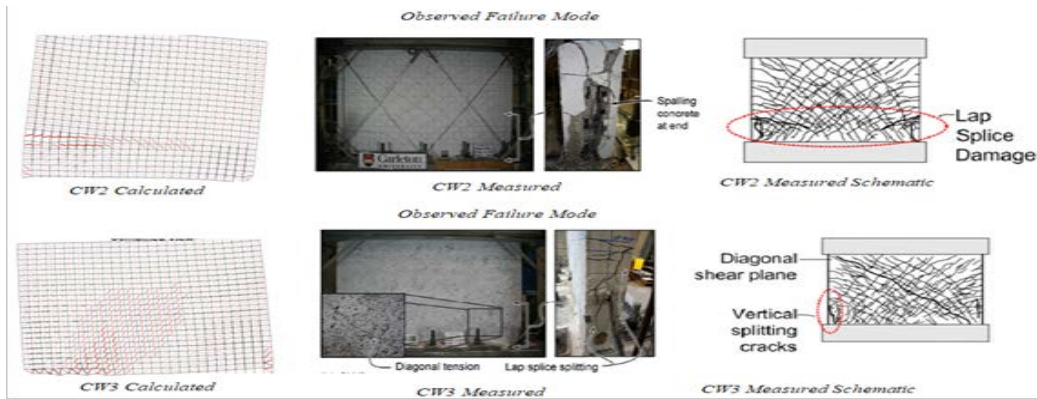


Figure 8. Control Wall Specimens Calculated vs. Measured Failure Modes

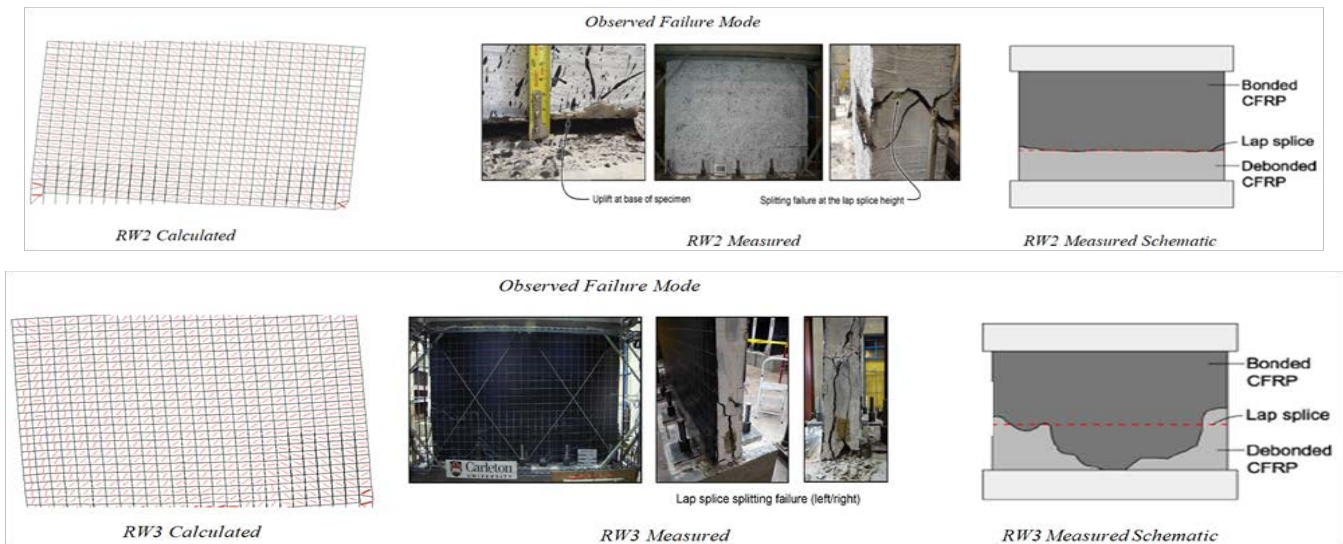


Figure 9. Repaired Wall Specimens Calculated vs. Measured Failure Modes

## PERFORMANCE OF THE CONTROL WALL SPECIMENS

As shown in Figures 6 and 7, the global response of the calculated control and repaired wall specimens show good agreement with their measured counterparts. In the control walls (CW1, CW2, CW3) the percentage difference in stiffness and strength is around 8%, ultimate displacement at 3% along with drift at 5%. The control wall specimens modes of failure are also in agreement with the experimental modes of failure shown in Figure 8. It is worth to note, that CW1 failed in diagonal tension shear with a crack formation initiating from the middle and then extending to the edge of the wall forming a failure plane as illustrated in Figure 8 (CW3 Schematic). CW2 on the other hand failed with the formation of a shear failure plane on top of the lap splice length of  $21d_b$ , which is clearly demonstrated in the analytical VT2 simulation. This failure signifies that the lap spliced bars experienced splitting failure prior to any flexural yielding in the bars or any formation of diagonal shear cracks. In addition to the horizontal shear failure plane, vertical splitting cracks on the edges of the wall specimen started to form indicating the loss of all associated bearing capacity between the concrete medium and the longitudinal bars. With respect to CW3, the mode of failure observed in the analytical simulation is the same as that of CW1, however the formation of splitting cracks at the end of the wall specimen indicates the slippage of the lapped bars at the end of the wall specimen.

## PERFORMANCE OF THE REPAIRED WALL SPECIMENS

The performance of the repaired wall specimens differed significantly from the behaviour of the control walls. Increases in load bearing capacity, ultimate displacement, and drift which in turn signify incremental increases in ductility and energy dissipation are evident (RW1 & RW3). On average the percentage difference in stiffness between the calculated (RW1, RW2, RW3) and measured amounts to 17%, ultimate strength, ultimate displacement and drift to 7%. The response for RW1 changed from a brittle shear failure as witnessed in CW1 to a flexural more ductile mode of failure by the formation of a sliding shear failure plane at the bottom of the wall. In contrast to the response typically observed in walls with no lap splices, RW2 and RW3 had notable trends and characteristics associated with their respective response and modes of failure. In RW2, the CFRP sheets are not able to restore the strength or stiffness of the wall specimen back to its original undamaged state. This is due to the excessive damage contracted by the lap splice due to the insufficient lap spliced length provided. Once the wall specimen reaches the ultimate load shown in Table 2, rapid bond degradation is witnessed and the shear failure plane ensues at the top of the lap splice. The FRP sheets start debonding from the bottom of the wall up to the shear failure plane simultaneously. With respect to RW3, the FRP retrofitting scheme is capable of restoring the strength of the specimen, as well as being able to transform the brittle behavior witnessed in the analytical simulation shown in Figure 8. to a more ductile behavior resulting in splitting vertical cracks at the edge of the wall specimen and the initiation of a sliding shear failure plane at the base of the wall.

## CONCLUSIONS

The main goal of this study is to gain insight of the behavior of squat reinforced concrete shear wall elements with deficiencies ranging from inadequate confinement, inadequate detailing, and the presence of non-ductile details (lap splice) at potential plastic hinge locations. The study investigates utilizing CFRP sheets to remedy design defects caused by the inclusion of lap spliced bars of different bonded length in plastic hinge regions of the wall specimens. The finite element simulation results show good estimate of the inelastic hysteresis behavior of the wall specimens under quasi-static reverse cyclic loading. The modelling process presented in this paper is effective in depicting the response of lap spliced bars in unconfined shear wall specimens. Key findings include: (a) The Harajli bond stress-slip model is effective in modeling the behavior of lap spliced bars in unconfined concrete shear wall specimens. (b) The IC debonding phenomenon is an important factor that should be considered in determining the maximum load bearing capacity and the non-linear response of the wall specimens. (c) The analysis software Vector2 can accurately simulate the repair of reinforced concrete shear walls with externally bonded FRP sheets. It can simulate the complex response of interactions between the FRP sheets and the concrete substrate as witnessed in this study. Future work will focus on proposing and modeling different retrofitting scenarios to improve the capacity of squat RC shear walls with insufficient lap splice length.

## ACKNOWLEDGMENTS

The ongoing research study is part of the Canadian Seismic Research Network (CSRN). The authors gratefully acknowledge the support provided by (CSRN).

## REFERENCES

- [1] ACI 318 (1968), "Building Code Requirements for Structural Concrete", American Concrete Institute, Detroit, Michigan, USA.
- [2] CSA (1977), "Code for the Design of Concrete Structures for Buildings", CAN3-A23.3-M77, Canadian Standard Association, Rexdale, Ontario, Canada.

- [3] ACI 318 (2014), "Building Code Requirements for Structural Concrete", American Concrete Institute, Farmington Hills, Michigan, USA.
- [4] CSA (2014), "Design of Concrete Structures", CSA A23.3-14, Canadian Standard Association, Rexdale, Ontario, Canada.
- [5] Paterson, J. and Mitchell, D. (2003), "Seismic Retrofit of Shear Walls with Headed Bars and Carbon Fiber Wrap", *Journal of Structural Engineering, ASCE, Vol. 129, No. 5, pp. 606-614.*
- [6] Khalil, A. and Ghobarah, A. (2005), "Behaviour of Rehabilitated Structural Walls." *J. of Earthquake Eng., (9)3, 371-391*
- [7] Layssi, H. and Mitchell, D. (2012), "Experiments on Seismic Retrofit and Repair of Reinforced Concrete Shear Walls", *Proceedings of the 6th International Conference on FRP Composites in Civil Engineering (CICE), June 13-15, 2012, Rome, Italy.*
- [8] Woods, J.E., Lau, D. T., Cruz-Noguez, C.A. (2016), "In-Plane Seismic Strengthening of NonDuctile Reinforced Concrete Shear Walls Utilizing Externally Bonded CFRP Sheets", *J. Comps. Construction, 10.1061/(ASCE) CC. 1943-5614,0000705.*
- [9] Wong, S. Y., and Vecchio, F. J. (2003), "Towards modeling of reinforced concrete members with externally bonded fiber-reinforced polymer composites", *ACI Struct. J., 100(1), 47-55.*
- [10] Lu, X. Z., Teng, J. G., Ye, L. P., and Jiang, J. J. (2007). "Intermediate crack debonding in FRP-strengthened RC beams: FE analysis and strength model." *J. of Comp. for Constr., ASCE, (11)2, 161-174.*
- [11] Teng, X. and Zhang, Y. (2014). "Nonlinear Finite Element Analyses of FRP-Strengthened Concrete Slabs under Fixed-Point Cyclic Loading." *J. Compos. Constr., 10.1061/(ASCE)CC.1943-5614.0000519, 04014057.*
- [12] Khomwan, N., Foster, S. J., and Smith, S. T. (2010). "FE modeling of FRP repaired planar concrete elements subjected to monotonic and cyclic loading." *J. Comp.Constr., 10.1061/(ASCE)CC.1943-5614.0000126, 720-729.*
- [13] Cortes, L., and Palermo, D. (2012). "Modeling of RC shear walls retrofitted with steel plates or FRP sheets." *J. Struct. Eng, 138(5), 602–612.*
- [14] Cruz-Noguez, C., Lau, D., and Sherwood, E. (2014), "Seismic Behaviour of RC Shear Walls with Externally Bonded FRP Sheets: Analytical Studies," *J. Comp.Constr., 10.1061/(ASCE)CC.1943-5614.0000466, 04014011.*
- [15] Teng, J. G., Chen, J. F., Smith, S. T., and Lam, L. (2002). FRP-strengthened RC structures, Wiley, London.
- [16] Wong, P. S., and Vecchio, F. J. (2002). VecTor2 and FormWorks user's manual (Publication No. 2002-02). Toronto, ON, Canada: University of Toronto, Department of Civil Engineering.
- [17] Shaheen, I. (2014), "Seismic Retrofit and Strengthening of Deficient Reinforced Concrete Shear Walls Using Externally Bonded Fibre Reinforced Polymer Sheets", Master's Thesis, Department of Civil and Environmental Engineering, Carleton University, Ottawa, Ontario.
- [18] Paulay T, Priestley MJN (1992): Seismic Design of Reinforced Concrete and Masonry Buildings, Wiley.
- [19] Eligehausen R, Popov EP, Bertero VV (1983), "Local bond stress-slip relationships of deformed bars under generalized excitations, Rep. UCB/EERC-83/23." Univ of Calif Berkeley, 162 pp.
- [20] Filippou FC, Popov EP, Bertero VV (1983), "Effects of bond deterioration on hysteretic behavior of reinforced concrete joints." Rep. UCB/EERC-83/19, Univ. of Calif., Berkeley, 184 pp.
- [21] Harajli M. H., Hamad B. S., Rteil A. (2004) "Effect of confinement on bond strength between steel bars and concrete." *ACI Structural Journal* 101(5): September-October, pp. 595–603.
- [22] Harajli, M. H., (2006), "Effect of confinement using steel, FRC, or FRP on the bond stress-slip response of steel bars under cyclic loading." *Materials and Structures., 39, 621–634.*
- [23] Cho, J.Y. and Pinchiera, J. (2004), "Nonlinear Modelling of RC Columns with Short Lap splices", 13th World Conference on Earthquake Engineering, Vancouver, British Columbia, Canada, August 2004.
- [24] Layssi, H. (2013), "Seismic Retrofit of Reinforced Concrete Shear Walls", Phd Dissertation, McGill University, Montréal, Quebec.
- [25] Melek, M., Wallace, J. W., and Conte, J. P. (2003), "Experimental Assessment of Columns with Short Lap Splices Subjected to Cyclic Load," *PEER Report 2003/04*, University of California, Berkeley. 73
- [26] Popovics, S. (1973), "A Numerical Approach to the Complete Stress-Strain Curve of Concrete", *Cement and Concrete Research, Vol. 3, No.5, pp. 583-599.*
- [27] Mander, J.B., Priestley, M.J.N., and Park. R., (1988). "Theoretical Stress-Strain Model for Confined Concrete", *ASCE Journal of Structural Engineering, Vol. 114, No. 8, pp. 1804-1826.*
- [28] Vecchio, F. J., and Lai, D. (2004), "Crack Shear-Slip in Reinforced Concrete Elements", *Journal of Advanced Concrete Technology, Vol. 2, No. 3, pp.289-300.*
- [29] Palermo, D., and Vecchio, F. J. (2002). "Behavior of three-dimensional reinforced concrete shear walls." *ACI Structural Journal, 99(1), 81-89.*
- [30] Woods, J. , Lau, D., Cruz-Noguez, C., Shaheen, I. (2017), "Repair of Earthquake Damaged Squat Reinforced Concrete Shear Walls using Externally Bonded CFRP Sheets", *16<sup>th</sup> World Conference on Earthquake Engineering, Santiago, Chile, January 9<sup>th</sup>-14<sup>th</sup>.*